

A New Single-Phase PLL Structure Based on Second Order Generalized Integrator

Mihai Ciobotaru, Remus Teodorescu and Frede Blaabjerg

Aalborg University
 Institute of Energy Technology
 Pontoppidanstraede 101, 9220 Aalborg
 DENMARK
mpc@iet.aau.dk, ret@iet.aau.dk, fbl@iet.aau.dk

Abstract – Phase, amplitude and frequency of the utility voltage are critical information for the operation of the grid-connected inverter systems. In such applications, an accurate and fast detection of the phase angle, amplitude and frequency of the utility voltage is essential to assure the correct generation of the reference signals and to cope with the new upcoming standards. This paper presents a new phase-locked-loop (PLL) method for single-phase systems. The novelty consists in generating the orthogonal voltage system using a structure based on second order generalized integrator (SOGI). The proposed structure has the following advantages: - it has a simple implementation; - the generated orthogonal system is filtered without delay by the same structure due to its resonance at the fundamental frequency, - the proposed structure is not affected by the frequency changes. The solutions for the discrete implementation of the new proposed structure are also presented. Experimental results validate the effectiveness of the proposed method.

I. INTRODUCTION

Phase, amplitude and frequency of the utility voltage are critical information for the operation of the grid-connected inverter systems. In such applications, an accurate and fast detection of the phase angle, amplitude and frequency of the utility voltage is essential to assure the correct generation of the reference signals and to cope with the new upcoming standards.

Most recently, there has been an increasing interest in Phase-Locked-Loop (PLL) topologies for grid-connected systems. The PLL is a grid voltage phase detection structure. In order to detect this phase an orthogonal voltage system is required. In single-phase systems there is less information than in three-phase systems regarding the grid condition, so more advanced methods should be considered in order to create an orthogonal voltage system [1]-[6].

The main task of a PLL structure is to provide a unitary power factor operation, which involves synchronization of the inverter output current with the grid voltage, and to give a clean sinusoidal current reference. Also using a PLL structure the grid voltage parameters, such as grid voltage amplitude and frequency, can be monitored. The grid voltage

monitoring is used to ensure that the performances of a grid-connected system comply with the standard requirements for operation under common utility distortions as line harmonics /notches, voltage sags/swells/loss, frequency variations and phase jumps.

The general structure of a single-phase PLL including the grid voltage monitoring is shown in Fig.1. Usually, the main difference among divers single-phase PLL methods is the orthogonal voltage system generation structure.

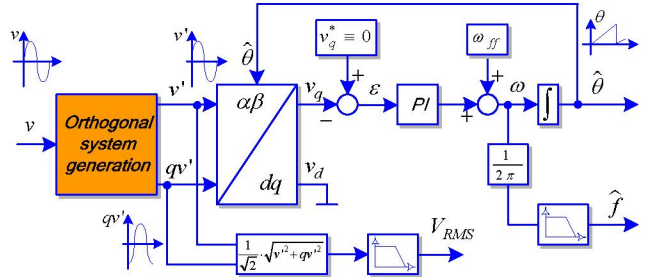


Fig. 1. General structure of a single-phase PLL

An easy way of generating the orthogonal voltage system in a single-phase structure is using a transport delay block, which is responsible for introducing a phase shift of 90 degrees with respect to the fundamental frequency of the input signal (grid voltage). A related method, but more complex of creating a quadrature signal is using the Hilbert transformation [3]. Another different method of generating the orthogonal voltage system is using an inverse Park Transformation as presented in [1], [3], [4] and [5]. All this methods has some shortcomings as follows: frequency dependency, high complexity, nonlinearity, poor or none filtering. Thus, further attention should be paid on single-phase PLL systems.

This paper presents a new method of single-phase PLL structure based on second order Generalized Integrator (GI). The proposed method is a good alternative for creating an orthogonal system in single-phase systems compared to known method [1]-[5]. This method is further presented and experimentally validated.

II. ORTHOGONAL SYSTEM GENERATION

The proposed method of creating an orthogonal system is depicted in Fig. 2. As output signals, two sine waves (v' and qv') with a phase shift of 90° are generated. The component v' has the same phase and magnitude as the fundamental of the input signal (v) [7].

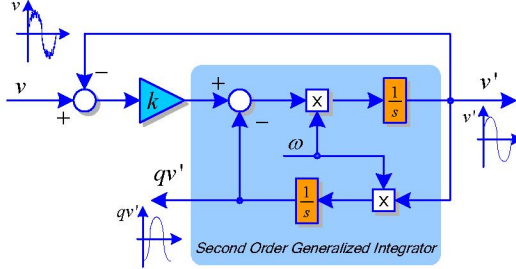


Fig. 2. General structure of a single-phase PLL

The presented structure is based on second order generalised integrator (SOGI), which is defined as [7]-[11]:

$$GI = \frac{\omega s}{s^2 + \omega^2} \quad (1)$$

- where ω represents the resonance frequency of the SOGI.

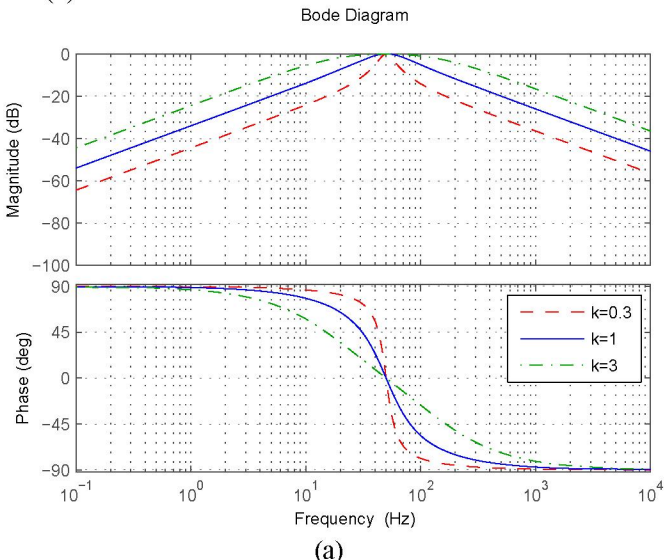
The closed-loop transfer functions ($H_d = \frac{v'}{v}$ and $H_q = \frac{qv'}{v}$) of the structure presented in Fig. 2 are defined as:

$$H_d(s) = \frac{v'}{v}(s) = \frac{k\omega s}{s^2 + k\omega s + \omega^2} \quad (2)$$

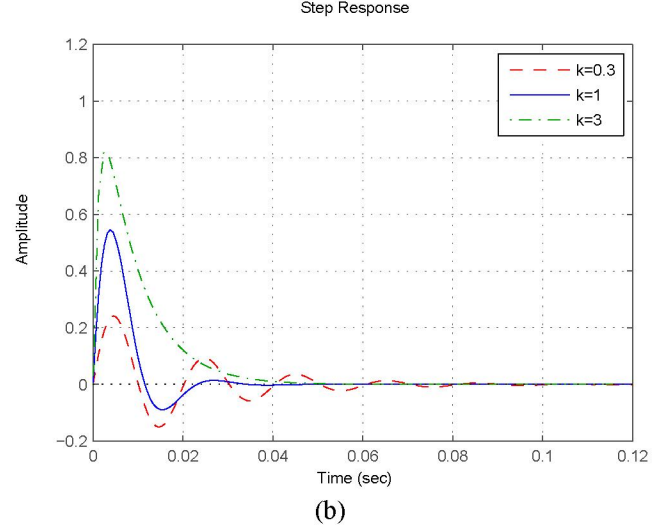
$$H_q(s) = \frac{qv'}{v}(s) = \frac{k\omega^2}{s^2 + k\omega s + \omega^2} \quad (3)$$

- where k affects the bandwidth of the closed-loop system.

The Bode representation and the step response of the closed-loop transfer function ($H_d = \frac{v'}{v}$) for the proposed structure at different values of gain k are shown in Fig. 3(a) and (b).



(a)



(b)

Fig. 3. Bode Plot (a) and Step Response (b) of the close-loop transfer function (H_d) at different values of gain k

The tuning of the proposed structure is frequency dependent, thus problems can occur when grid frequency has fluctuations. As a consequence, an adaptive tuning of the structure in respect to its resonance frequency is required. Therefore, the resonance frequency value of the SOGI is adjusted by the provided frequency of the PLL structure.

The proposed method for creating the orthogonal system has a main advantage compared to known methods (i.e. Transport-Delay, Hilbert Transformation, and Inverse Park Transformation) [1]-[5]. Only using a simple structure, as it can be seen from Fig. 2, three main tasks are performed: - generating the orthogonal voltage system; - filtering the orthogonal voltage system without delay; - the structure is frequency adaptive.

Using the proposed method the input signal v (grid voltage) is filtered resulting two clean orthogonal voltages waveforms v' and qv' , due to the resonance frequency of the SOGI at ω (grid frequency). The level of filtering can be set from gain k as follows: - if k decreases the bandpass of the filter becomes narrower resulting a heavy filtering, but in the same time the dynamic response of the system will become slower as it can be observed from Fig. 3(b). As it can be seen from Fig. 3(a), at resonance frequency there is no attenuation compared to a quite large attenuation outside this frequency.

An example about how it works this method is presented in Fig. 4. The effect of the filter is depicted with a distorted grid voltage waveform (V_g) containing notches. The created orthogonal system is represented of v' and qv' . For this experimental result the gain k was equal to 0.8.

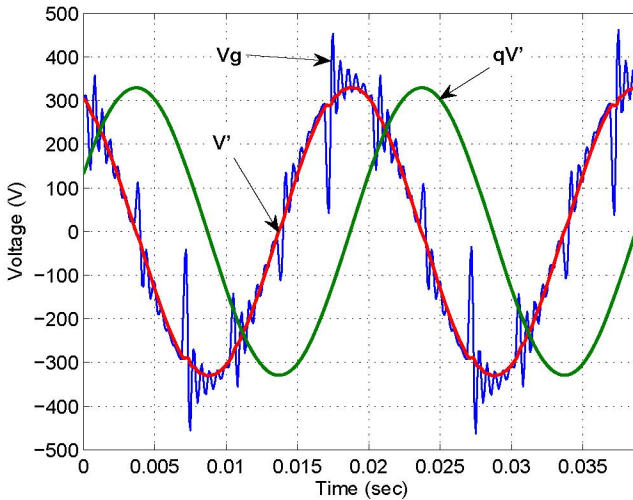


Fig. 4. Distorted grid voltage V_g and generated orthogonal voltage system (V' and its quadrature qV')

III. DISCRETISATION OF THE SOGI

The discrete implementation of the orthogonal system generation structure based on SOGI is described in the following.

The Euler method is the most used common method in order to obtain a Discrete-Time Integrator. The equations of this method are presented below:

Forward Euler method:

$$y(n) = y(n-1) + T_s u(n-1)$$

For this method, $\frac{1}{s}$ is approximated by:

$$T_s \frac{z^{-1}}{1-z^{-1}} \quad (4)$$

Backward Euler method:

$$y(n) = y(n-1) + T_s u(n)$$

For this method, $\frac{1}{s}$ is approximated by:

$$T_s \frac{1}{1-z^{-1}} \quad (5)$$

The structure presented in Fig. 2 can be easily implemented in a discrete form using the Forward Euler method for the first integrator (its output is v') and the Backward Euler method for the second integrator (its output is qv') in order to avoid an algebraic loop. It is also known that the Discrete-Time Integrator using Euler method does not have an ideal phase of -90 degrees.

The phases for the Forward Euler, Backward Euler and Trapezoidal methods at different frequencies are shown in Fig. 5. The sampling time (T_s) was set to 10^{-4} . It can be noticed that at 50 Hz the Forward and Backward Euler methods do not provide a phase of -90 degrees. Therefore, the two outputs (v' and qv') of the orthogonal system generation structure presented in Fig. 2 will not be exactly in quadrature.

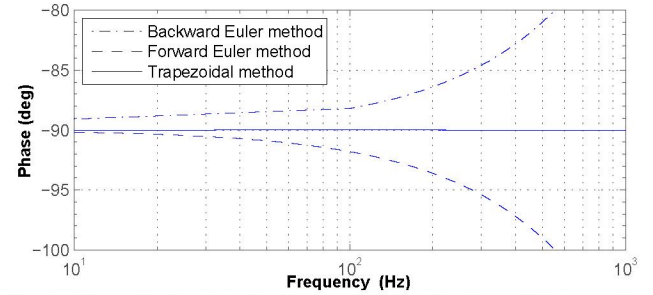


Fig. 5. Phase Bode plots for Forward Euler, Backward Euler and Trapezoidal methods

Due to the fact that qv' is not 90 degrees phase shifted by v' , a ripple of 100 Hz will appear in the estimated amplitude and frequency of the input signal as it can be seen from Fig. 6. The input signal was a clean sinusoid with a frequency of 50 Hz and 325 units amplitude.

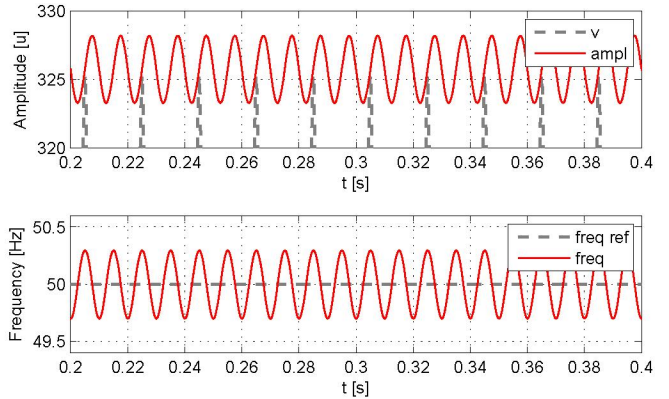


Fig. 6. Estimated amplitude and frequency of the input signal when Euler method is used

However, the solution for this inconvenience is to make use of more advanced numerical methods for the Discrete-Time Integrator. Thus, three different methods are described in the following:

- *Trapezoidal method;*
- *Second order integrator;*
- *Third order integrator;*

A. Trapezoidal method

The equation of the integrator using this method is presented below:

$$y(n) = y(n-1) + \frac{T_s}{2} [u(n) + u(n-1)]$$

For this method, $\frac{1}{s}$ is approximated by:

$$\frac{T_s}{2} \frac{1+z^{-1}}{1-z^{-1}} \quad (6)$$

As it can be seen from Fig. 5 a phase of -90 degrees can be obtained using Trapezoidal method for the whole spectrum of frequencies. Anyway, the Trapezoidal method can not be applied just replacing $\frac{1}{s}$ from Fig. 2 with (6), because an

algebraic loop will issue. Therefore, the solution is to use the Trapezoidal method for the close-loop transfer function ($H_d = \frac{v'}{v}$) presented in (2) in order to avoid any other algebraic loops.

Replacing s by $\frac{2}{T_s} \frac{z-1}{z+1}$, in (2) will result:

$$H_0(z) = \frac{k\omega \frac{2}{T_s} \frac{z-1}{z+1}}{\left(\frac{2}{T_s} \frac{z-1}{z+1}\right)^2 + k\omega \frac{2}{T_s} \frac{z-1}{z+1} + \omega^2} \quad (7)$$

Solving further the equation it results:

$$H_0(z) = \frac{(2k\omega T_s)(z^2 - 1)}{4(z-1)^2 + (2k\omega T_s)(z^2 - 1) + (\omega T_s)^2(z+1)^2} \quad (8)$$

Making the following substitutions $\begin{cases} x = 2k\omega T_s \\ y = (\omega T_s)^2 \end{cases}$ and

bringing the equation to a canonical form it will result:

$$H_0(z) = \frac{\left(\frac{x}{x+y+4}\right) + \left(\frac{-x}{x+y+4}\right)z^{-2}}{1 - \left(\frac{2(4-y)}{x+y+4}\right)z^{-1} - \left(\frac{x-y-4}{x+y+4}\right)z^{-2}} \quad (9)$$

$$\text{Substituting } \begin{cases} b_0 = \frac{x}{x+y+4} \\ b_2 = \frac{-x}{x+y+4} = -b_0 \end{cases} \text{ and } \begin{cases} a_1 = \frac{2(4-y)}{x+y+4} \\ a_2 = \frac{x-y-4}{x+y+4} \end{cases},$$

a simple discrete form of (2) is obtained:

$$H_d(z) = \frac{b_0 + b_2 z^{-2}}{1 - a_1 z^{-1} - a_2 z^{-2}} \quad (10)$$

Furthermore, (9) can be represented as follows:

$$H_d(z) = b_0 \cdot \frac{1 - z^{-2}}{1 - a_1 z^{-1} - a_2 z^{-2}} \quad (11)$$

The implementation of the Trapezoidal method using (11) is depicted in Fig. 7, where $w = 2T_s\omega$.

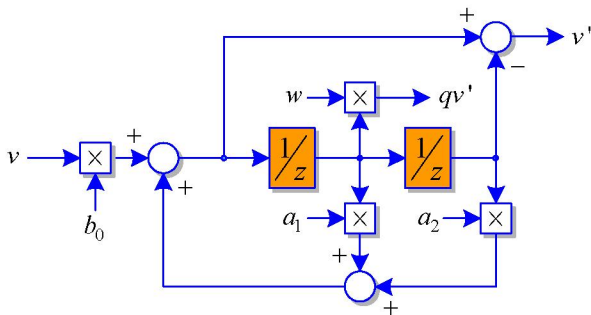


Fig. 7. Trapezoidal method implementation

B. Second order integrator

The equation of the second order integrator is presented below [12]:

$$y(n) = y(n-1) + \frac{T_s}{2} [3u(n-1) - u(n-2)]$$

For this method, $\frac{1}{s}$ is approximated by:

$$\frac{T_s}{2} \frac{3z^{-1} - z^{-2}}{1 - z^{-1}} \quad (12)$$

The implementation of the second order using (12) integrator is presented in Fig. 8.

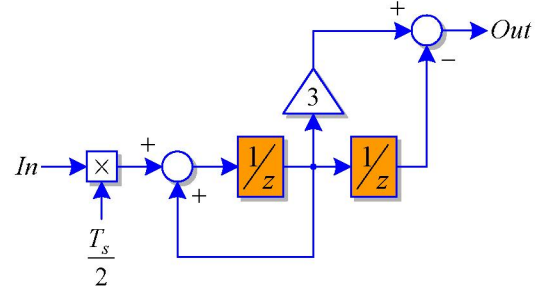


Fig. 8. Second order integrator implementation

C. Third order integrator

The equation of the third order integrator is given in the following [12]:

$$y(n) = y(n-1) + \frac{T_s}{12} [23u(n-1) - 16u(n-2) + 5u(n-3)]$$

For this method, $\frac{1}{s}$ is approximated by:

$$\frac{T_s}{12} \frac{23z^{-1} - 16z^{-2} + 5z^{-3}}{1 - z^{-1}} \quad (13)$$

Fig. 9 shows the implementation of the third order integrator.

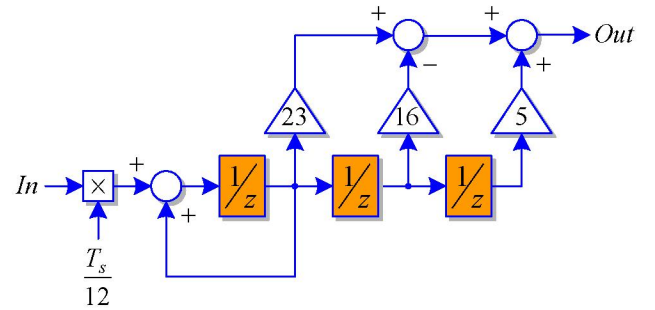


Fig. 9. Third order integrator implementation

In Fig. 10, a comparison between the Trapezoidal Method (T), second order integrator (2) and third order integrator (3) is made. As it can be noticed, the best results are obtained when the third order integrator is used. Anyway, the all three proposed solutions give very good results compared to the Euler method.

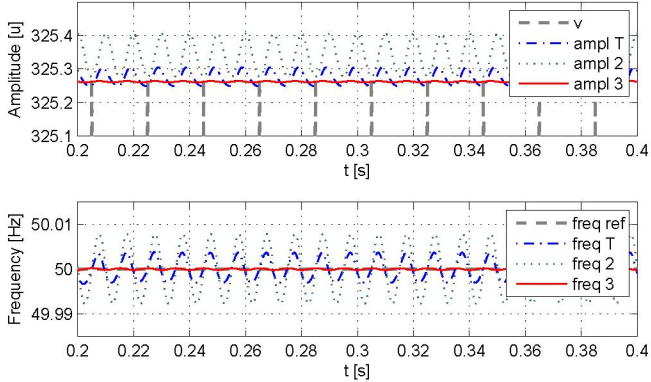


Fig. 10. Estimated amplitude and frequency of the input signal when Second order integrator, Third order integrator and Trapezoidal method are used

IV. EXPERIMENTAL RESULTS

An experimental system using a grid simulator (5kVA AC Power Source – model 5001 ix - California Instruments) has been built in order to test the proposed structure. The control structure was implemented using dSPACE 1103 platform.

The proposed PLL structure based on second order generalized integrator is experimentally validated in the following.

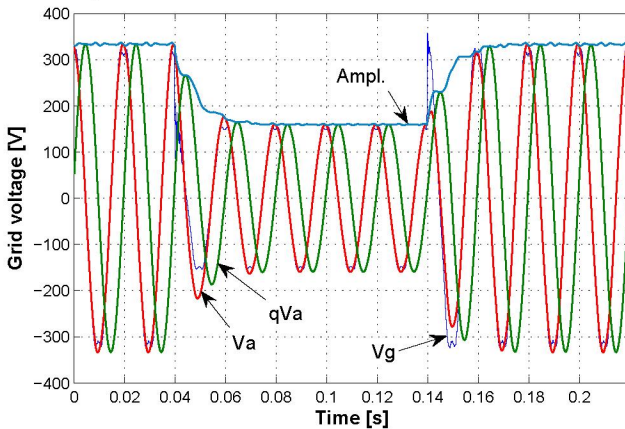


Fig. 11. Grid voltage sag of 50% - 10% THD ($k=0.8$)

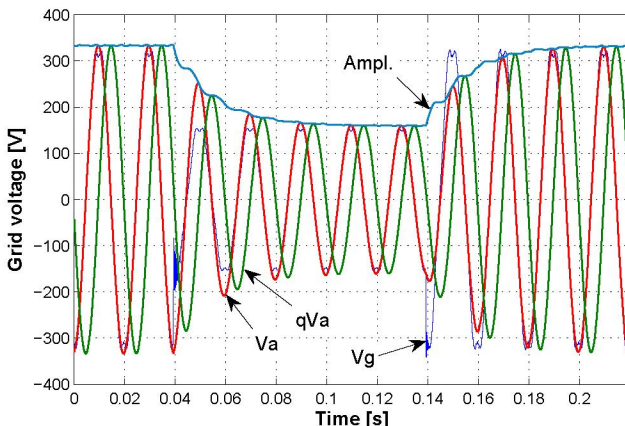


Fig. 12. Grid voltage sag of 50% - 10% THD ($k=0.4$)

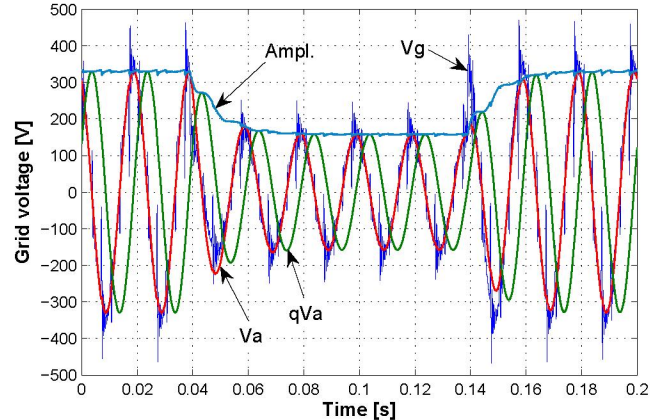


Fig. 13. Grid voltage sag of 50% - Notches ($k=0.8$)

All the experimental results were obtained using the PLL structure presented in Fig. 1. The block “Orthogonal system generation” was replaced with the structure presented in Fig. 2. For all experimental results presented in this paper, the PI controller parameters of the PLL structure were set as follows: - the settling time $T_{set}=0.06$ s; - damping factor $\xi=1$. All the measurements have been done without using additional filters.

Fig. 11, 12 and 13 show the behaviour of the PLL system based on SOGI under grid voltage sag of 50%. The effect of the gain k (Fig. 2) at two different values is depicted in Fig. 11 and 12 for a grid voltage THD of 10%. It can be noticed that a smaller value of the gain gives a better filtering but slows the dynamic of the system. In Fig. 13 the proposed PLL structure is tested under a high content of notches in the grid voltage.

Fig. 14 and 15 show a frequency step and sweep response from 50 up to 51 Hz. It can be observed a fast estimation of the grid frequency. The grid voltage THD was set to 3% for this experiment.

The PLL behaviour under a phase jump of 60 degrees and voltage sag of 25% is presented in Fig. 16. It can be noticed that the PLL system responds according to its settling time ($T_{set}=0.06$ s).

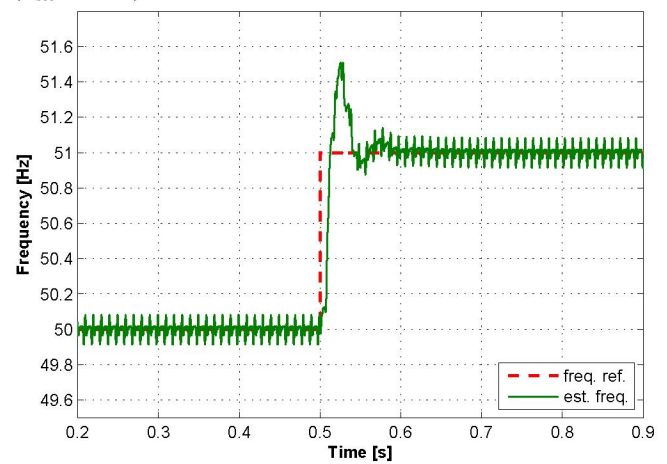


Fig. 14. Grid frequency step from 50 to 51 Hz ($k=0.8$)

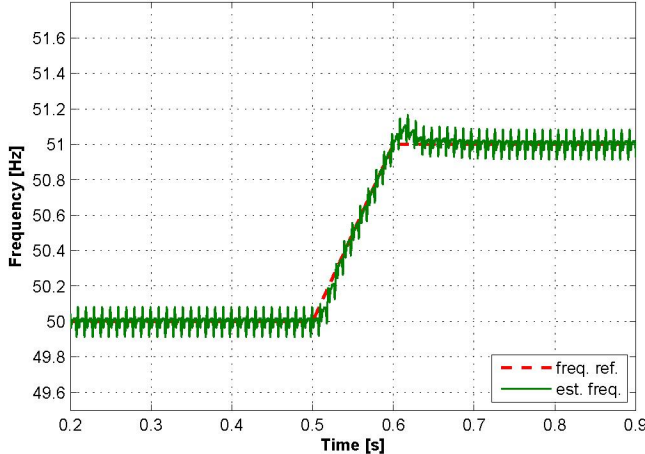


Fig. 15. Grid frequency sweep from 50 to 51 Hz ($k=0.8$)

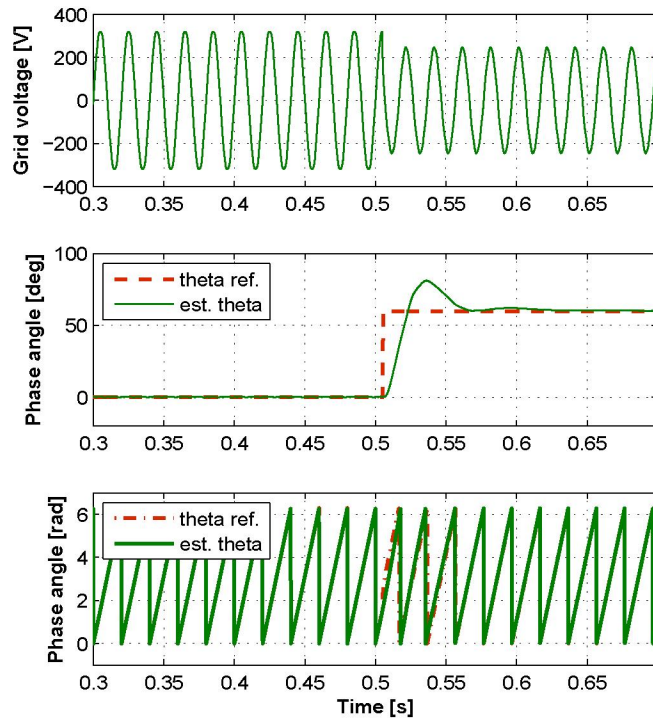


Fig. 16. Phase jump of 60 degrees and voltage sag of 25%

V. CONCLUSIONS

In this paper, a new single-phase PLL structure based on second order generalised integrator is presented. Using the known vectorial approach for the three phase systems, a new algorithm for single-phase systems was derived. The proposed structure has the following advantages: - it has a simple implementation; - the generated orthogonal system is filtered without delay by the same structure due to its resonance at the fundamental frequency, - the proposed structure is not affected by the frequency changes. The solutions for the discrete implementation of the new proposed structure are also presented. The effectiveness of the proposed method has been validated by the experimental results.

VI. REFERENCES

- [1] L.N. Arruda, S.M. Silva, B.J.C. Filho, "PLL structures for utility connected systems", *Industry Applications Conference IAS*, 2001, vol. 4, pp. 2655 – 2660.
- [2] N. Saitou, M. Matsui, and T. Shimizu, "A Control Strategy of Single-phase Active Filter using a Novel d-q Transformation", *Industry Applications Society IAS*, 2003, pp. 1222-1227.
- [3] S.M. Silva, B.M. Lopes, B.J.C. Filho, R.P. Campana, "Performance evaluation of PLL algorithms for single-phase grid-connected systems", *Industry Applications Conference*, 2004, vol.4, pp. 2259 - 2263.
- [4] S.M. Silva, L.N. Arruda, and B.J.C. Filho, , "Wide Bandwidth Single and Three-Phase PLL Structures for Utility Connected Systems", *9th. European Conference on Power Electronics and Applications EPE*, 2001, pp. 1660-1663.
- [5] M. Ciobotaru, R. Teodorescu , F. Blaabjerg, "Improved PLL structures for single-phase grid inverters", *Proc. of PELINCEC'05*, 6 pages, paper ID 106.
- [6] M. Ciobotaru, R. Teodorescu , F. Blaabjerg, "Control of single-stage single-phase PV inverter", *Proc. of EPE'05*, 10 pages, ISBN : 90-75815-08-5.
- [7] B. Burger and A. Engler, "Fast signal conditioning in single phase systems" – *Proc. of European Conference on Power Electronics and Applications*, 2001.
- [8] X. Yuan, W. Merk, H. Stemmler and J. Allmeling, "Stationary-Frame Generalized Integrators for Current Control of Active Power Filters with Zero Steady-State Error for Current Harmonics of Concern Under Unbalanced and Distorted Operating Conditions" *IEEE Trans. on Ind. App.*, Vol. 38, No. 2, 2002, pp. 523 – 532.
- [9] R. Teodorescu, F. Blaabjerg, M. Liserre and U. Borup, "A New Control Structure for Grid-Connected PV Inverters with Zero Steady-State Error and Selective Harmonic Compensation", *Proc. of APEC'04*, Vol. 1, 2004, pp. 580-586.
- [10] S. Fukuda and T. Yoda, "A novel current-tracking method for active filters based on a sinusoidal internal mode", *IEEE Trans. on Ind. App.*, Vol.37, No. 3, 2001, pp. 888 – 895.
- [11] D. N. Zmood and D. G. Holmes, "Stationary Frame Current Regulation of PWM Inverters with Zero Steady-State Error", *IEEE Trans. on Power Electronics*, Vol. 18, No. 3, May 2003, pp. 814 – 822.
- [12] E. Ceangă, C. Nichita, L. Protin and N. A. Cutululis, "Théorie de la commande des systèmes", *Editura Tehnică Bucharest*, 2001, ISBN 973- 31-2103-7.